

Numerical Study on the Chaotic Response of the Minimal Chemical Oscillator to a Sinusoidal Perturbation

Yoshihiro Sasaki

Institute for Chemical Research, Kyoto University, Uji, Kyoto 611-0011

(Received April 5, 1999)

The chaotic response of the minimal chemical oscillator stimulated by a sinusoidal perturbation was studied by a computer-simulation method. Chaotic phase diagrams were obtained and two types of chaos were estimated. One was neighbored by fundamental 1/2 and fundamental 1/3 entrainment regions, and was followed by a quasiperiodic region. It contained two chaotic modes (relatively large-amplitude mode and relatively small-amplitude one on the Poincaré section ($\cos \omega_p t = 1$)) and coexisted with the fundamental 1/3 harmonic mode. Other chaotic regions appeared when fundamental 1/1 and fundamental 1/2 entrainment regions came into contact with each other, and these were not in contact with any quasiperiodic regions. In this case Hopf bifurcations from the fundamental 1/1 harmonic mode to the $1/n$ (n/n) (n : integer) harmonic modes occurred first, and were followed by chaotic modes between the harmonic modes and the $1/n$ ($(n-1)/n$) harmonic ones. The coexistence of the chaotic mode and the 1/3 harmonic mode and the existence of two chaotic modes were compared with the behaviors of a one-dimensional dynamical system having a piecewise linear map.

Chaos is of interest in many fields because of its strange behavior. It has also been reported in chemical systems, such as Belousov–Zhabotinski (BZ) and peroxidase–oxidase (PO) reactions.¹ The routes to chaos (period-doubling cascade, intermittency, etc.) have been mainly reported. In BZ and PO reaction systems, mixed-mode oscillations and chaos created through the oscillatory mode have often been observed. Hauser and Olsen have reported on the existence of a homoclinic-type chaos in a PO reaction.² Hauck and Schneider have observed a quasiperiodic route to chaos.³ The characteristics of chaotic behaviors and the phase diagrams on chaos have been studied rather poorly.

It is thought that nonlinear reaction systems stimulated by external forces would exhibit chaos. Kai and Tomita simulated chaos in a forced Brusselator for the first time.⁴ Chaos generated by stimulating neurons electrically were reported and their behaviors were simulated by using the Hodgkin–Huxley model.^{5,6} Dolnik et al. studied the BZ reaction in oscillatory and excitable modes forced by single or periodic perturbations and simulated by using models based on the Field–Körös–Noyes (FKN) mechanism.⁷

The reduction of bromate in an acidic medium, which is a part of the BZ reaction, is known to proceed via the FKN mechanism.⁸ The reaction system exhibits chemical oscillations with a small amplitude in a continuous-flow stirred tank reactor (CSTR), which is called the minimal oscillator.⁹ The FKN mechanism is known to reproduce the nonlinear behaviors (bistability, sustained oscillations, etc.) of the reaction system, which gives merit to studying various nonlinear properties of the reaction system.^{10,11} The author numerically studied the response of the minimal chemical oscillator to a sinusoidal perturbation over wide ranges of perturbation parameters.¹² The outline of the study was as follow:

Under weakly perturbed conditions, fundamental and secondary entrainments, quasiperiodicity, the Farey tree, and Arnol'd tongues were estimated; under more strongly perturbed conditions chaos, small-amplitude oscillations, and the coexistence of two oscillatory modes joined. Regarding chaos, two types of chaos were simulated. These complex behaviors under the relatively strong perturbations would be understood in the term, chaos. We studied the details of the chaotic response of a forced minimal chemical oscillator, and will report on the results in this paper.

Calculations

In this study we used rate equations derived from the FKN mechanism (Table 1) and the rate constants prepared by Field and Försterling.¹³ Because the reaction system was assumed to be studied in a CSTR, the terms $k_0(C_{0i} - C_i)$ were added to the rate equations, where C_i and C_{0i} represent the concentrations of species i in solution and in the feed flow, respectively and k_0 is the reciprocal of the residence time. The external parameters for the system in a CSTR were $[\text{BrO}_3^-]_0$, $[\text{Br}^-]_0$, $[\text{Ce}^{3+}]_0$, $[\text{H}^+]_0$, k_0 , and temperature. The values of $[\text{BrO}_3^-]_0$, $[\text{Br}^-]_0$, $[\text{Ce}^{3+}]_0$, $[\text{H}^+]_0$, and the temperature were fixed and k_0 was assumed to be varied sinusoidally,

Table 1. Reaction Mechanism of the Minimal Chemical Oscillator

$\text{Br}^- + \text{HBrO} + \text{H}^+ \rightleftharpoons \text{Br}_2 + \text{H}_2\text{O}$
$\text{Br}^- + \text{HBrO}_2 + \text{H}^+ \rightarrow 2\text{HBrO}$
$\text{Br}^- + \text{BrO}_3^- + 2\text{H}^+ \rightleftharpoons \text{HBrO} + \text{HBrO}_2$
$2\text{HBrO}_2 \rightarrow \text{HBrO} + \text{BrO}_3^- + \text{H}^+$
$\text{HBrO}_2 + \text{BrO}_3^- + \text{H}^+ \rightleftharpoons 2\text{BrO}_2\cdot + \text{H}_2\text{O}$
$\text{Ce}^{3+} + \text{BrO}_2\cdot + \text{H}^+ \rightleftharpoons \text{Ce}^{4+} + \text{HBrO}_2$

$$k_0 = \bar{k}_0(1 + \alpha \sin \omega_p t). \quad (1)$$

The values of \bar{k}_0 , being the average of k_0 , and the other external parameters used are listed in Table 2.

The temporal evolution of the reaction system was calculated by Gear's method. The results calculated up to 10^4 s were ordinarily discarded to remove any influence of the initial values. The discarding time was 3×10^5 s at its maximum when a slowing down occurred. The state of the system was evaluated by considering the shapes of Poincaré section ($\cos \omega_p t = 1$) and the Fourier spectra.¹⁴ The representation for the entrained modes used in this paper was the same as that in a previous paper.¹²

Results and Discussion

As described in the previous paper, the minimal oscillator stimulated by the sinusoidal perturbation exhibited two types of chaos. One appeared in the case that fundamental 1/2 and fundamental 1/3 entrainment regions began to come into contact with each other. The other was generated in the case that fundamental 1/1 and fundamental 1/2 entrainment regions began to do so. In this study, we investigated the for-

mer, which we call chaos of type I, in detail under condition A in Table 2 and the latter (chaos of type II) under condition B, respectively.

Chaos of Type I. Figure 1 shows a phase diagram on the chaos of type I in the ω_p - α plane. The chaotic region between the fundamental 1/2 and the fundamental 1/3 entrainment regions was also in contact with a quasiperiodic one. Therefore, there were three routes to the chaotic mode: (1) from the 1/2 harmonic mode, (2) from the 1/3 harmonic mode, and (3) from the quasiperiodic mode. The first transition (route 1) proceeded through successive period-doubling bifurcations (Fig. 1). The Feigenbaum ratio was 4.7 under the condition that $\alpha = 0.15$. The second transition (route 2) proceeded through an intermittent route. These routes have generally been observed in many reaction systems. The determination of route 3 (from quasiperiodic mode to chaotic mode) is rather difficult. Therefore, we discuss this route in Figs. 2 and 3, where the left figures are the oscillation patterns of $[\text{Ce}^{4+}]$, the middle ones their Fourier spectra, and right ones their Poincaré sections ($\cos \omega_p t = 1$). Figure 2 shows the dependency of the $[\text{Ce}^{4+}]$ oscillations with the ω_p value under the condition that $\alpha = 0.1$. Figure 2a' and 2a'' ($\omega_p = 0.05095 \text{ rad s}^{-1}$) reveal typical chaotic characters (a band-shaped Fourier spectrum and a collapse of the torus), and corrugations on the Poincaré section can be observed in Fig. 2b'' ($\omega_p = 0.05112 \text{ rad s}^{-1}$). On the other hand, the Poincaré sections in Fig. 2c'', 2d'', and 2e'' ($\omega_p = 0.0521$, 0.0526, and 0.0527 rad s^{-1} , respectively) are smooth, suggesting quasiperiodicity of the system. The peaks in the Fourier spectra of Fig. 2c' and 2d' are more distinct than those of Fig. 2a', suggesting that the chaotic character is

Table 2. Reaction Conditions for CSTR^{a)}

	Condition A	Condition B
$[\text{H}^+]_0$	0.75 M	
$[\text{Ce}^{3+}]_0$	3×10^{-4} M	
$[\text{Br}^-]_0$	2.9×10^{-4} M	
$[\text{BrO}_3^-]_0$	0.1 M	0.12 M
\bar{k}_0	0.005 s^{-1}	0.0064 s^{-1}

a) $1 \text{ M} = 1 \text{ mol dm}^{-3}$.

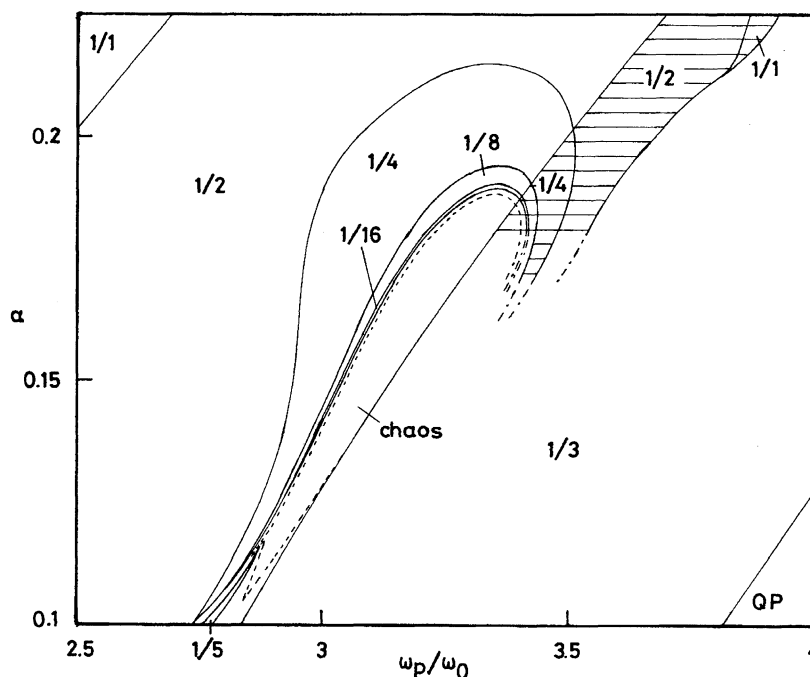


Fig. 1. Phase diagram on the chaos (type I) of the minimal chemical oscillator in the ω_p - α space. The CSTR condition: A ($[\text{BrO}_3^-]_0 = 0.1 \text{ M}$ ($1 \text{ M} = 1 \text{ mol dm}^{-3}$), and $\bar{k}_0 = 0.005 \text{ s}^{-1}$). QP: quasiperiodic oscillations. The striped pattern represents the region where the 1/3 fundamental harmonic mode and other harmonic modes coexist.

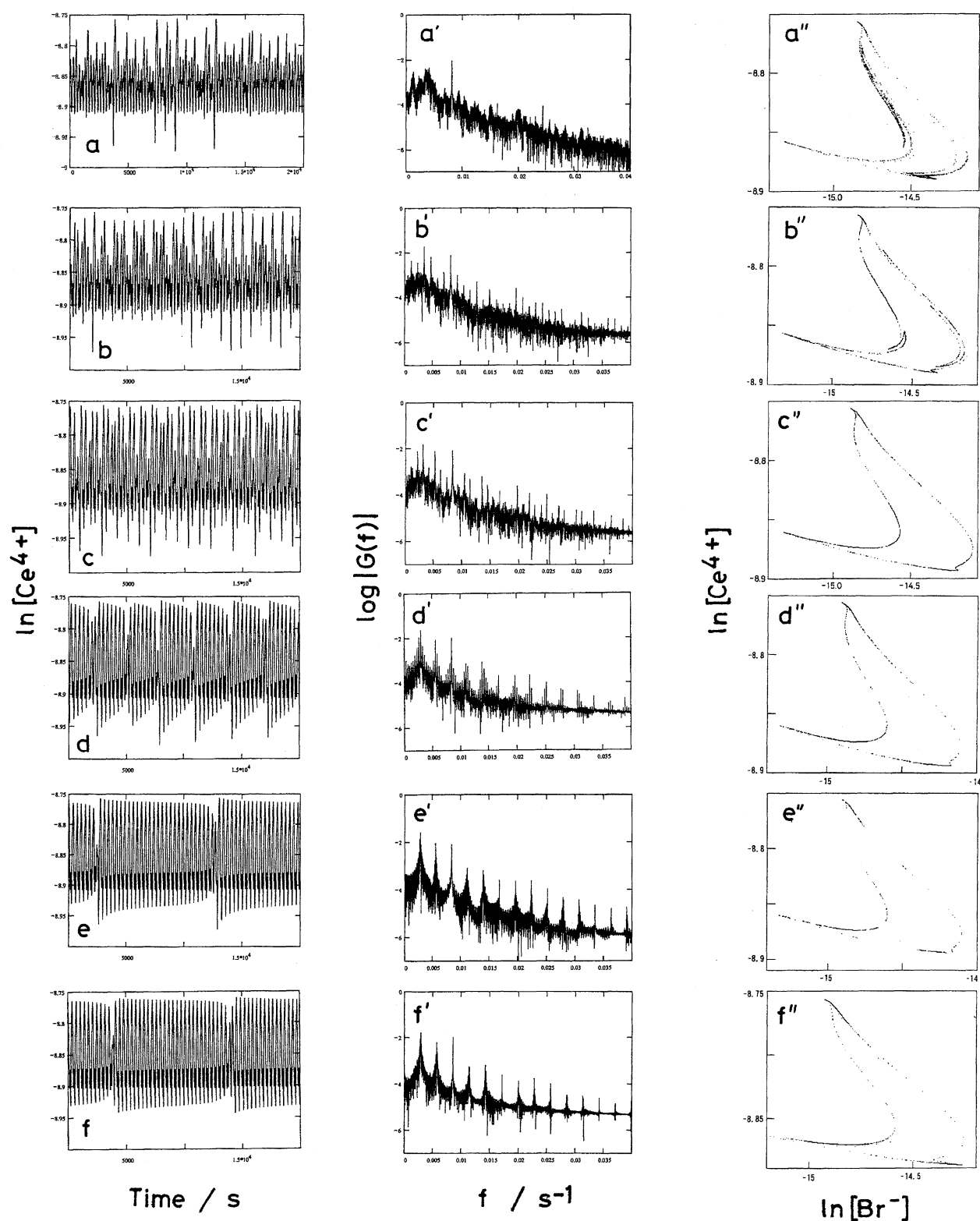


Fig. 2. Characteristics of oscillations of $[\text{Ce}^{4+}]$ under the condition that $\alpha = 0.1$. The CSTR condition: A. a (oscillation pattern), a' (Fourier spectrum), and a'' (Poincaré section ($\cos \omega_p t = 1$)): $\omega_p = 0.05095$. b, b', and b'': $\omega_p = 0.05112$. c, c', and c'': $\omega_p = 0.0521$. d, d', and d'': $\omega_p = 0.0526$. e, e', and e'': $\omega_p = 0.0527$. f, f', and f'': $\alpha = 0.11$ and $\omega_p = 0.05377$. The unit of the ω_p values is rad s^{-1} .

rather weak in Figs. 2c' and 2d'. (Also see Fig. 3c'''.) Figures 2e and 2e' revealed the characteristic of an intermittent chaos from the 1/3 harmonic mode. Figures 2f and 2f'

($\alpha = 0.11$ and $\omega_p = 0.05377 \text{ rad s}^{-1}$) also reveal the characteristic of intermittent chaos, and some dots appear inside the torus, as shown in Fig. 2f''. The inside dots may result from

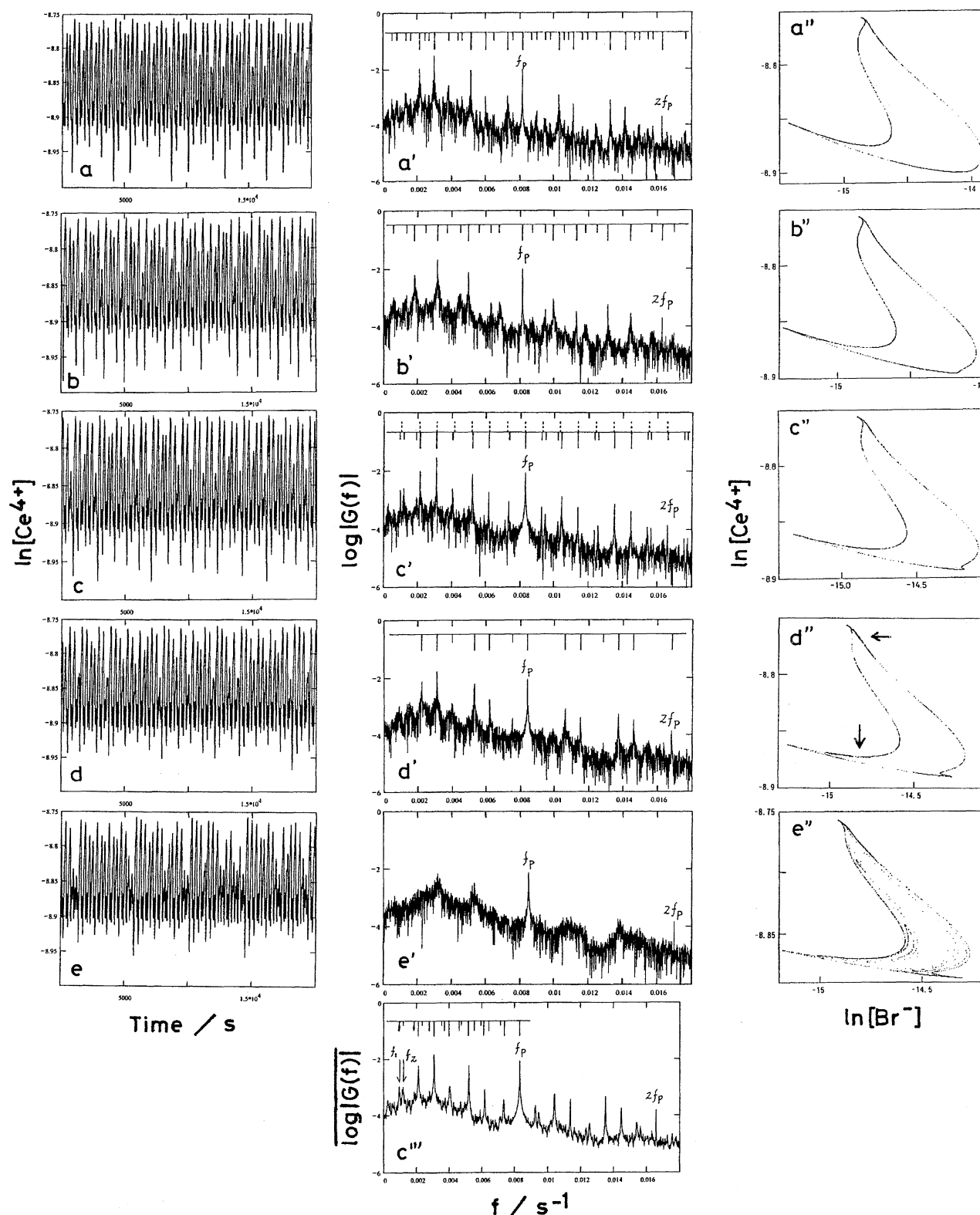


Fig. 3. Quasiperiodic route of the chaos of type I. The CSTR condition: A. a (oscillation pattern of $[\text{Ce}^{4+}]$), a' (Fourier spectrum), and a'' (Poincaré section ($\cos \omega_p t = 1$)): $\alpha = 0.09$ and $\omega_p = 0.05115$. b, b', and b'': $\alpha = 0.095$ and $\omega_p = 0.05115$. c, c', c'' (Fourier spectrum) and c'': $\alpha = 0.1$ and $\omega_p = 0.0521$. d, d', and d'': $\alpha = 0.105$ and $\omega_p = 0.0528$. e, e', and e'': $\alpha = 0.11$ and $\omega_p = 0.0534$. The unit of the ω_p values is rad s^{-1} . The Fourier spectrum c''' is an average over time series sampled in different manners.

corrugations on the Poincaré section. We thus concluded that the state of the system is chaotic in the cases of Figs. 2a, 2b, and 2f. However, we could not determine the state of the

system (either quasiperiodic state or chaotic one) in the cases of Figs. 2c, 2d, and 2e. This obscure determination was also caused by the following result calculated under the condition

that $\omega_p = 0.0521 \text{ rad s}^{-1}$: Two trajectories estimated from neighboring initial values separated after about $3.3 \times 10^4 \text{ s}$.¹⁵ If we could estimate the Liapunov exponents, positive values might be obtained. Figure 3 shows the dependency of the oscillation pattern of $[\text{Ce}^{4+}]$ on the magnitude of α in the condition that $\alpha \equiv 0.1$. The Poincaré sections in Figs. 3a'', 3b'', and 3c'' ($(\alpha, \omega_p \text{ (rad s}^{-1})) = (0.09, 0.05115), (0.095, 0.05115), \text{ and } (0.1, 0.0521)$, respectively) are smooth. The Poincaré section in Fig. 3d'' ($(\alpha, \omega_p \text{ (rad s}^{-1})) = (0.105, 0.0528)$) contains some dots inside at arrow points, and that in Fig. 3e'' ($(\alpha, \omega_p \text{ (rad s}^{-1})) = (0.11, 0.0534)$) is obviously collapsing. In the Fourier spectra the peaks of the perturbation frequency (f_p) and its higher harmonics are always observed. The Fourier spectra in Figs. 3a', 3b', 3c', and 3d' comprise broadband components and incommensurate peaks, whose positions are shown in upper parts of the figures. (Compare the positions of the peaks with those of the peaks due to $f_p/8$ frequency (dashed lines in Fig. 3c').) As shown in Fig. 3c''', the broadband components (maybe resulting from the chaotic character) are diminished and the incommensurate peaks became clear by averaging the differently sampled time series (20 samples). The peaks were reproduced by linear combinations of two frequencies ($f_1 (=f_p/9)$ and $f_2 (=f_p/7)$), as shown in the upper part of Fig. 3c'''. On the other hand, the Fourier spectrum in Fig. 3e'

exhibits only broadband components, except for the f_p and the $2f_p$ peaks. We thus concluded that the reaction system existed in a chaotic state under the conditions of Figs. 3d and 3e. Two trajectories calculated under the same condition as described above separated after about $5.4 \times 10^4 \text{ s}$ in the case of Fig. 3a and after about $5 \times 10^3 \text{ s}$ in the case of Fig. 3e. When $\alpha = 0.08$ and $\omega_p = 0.0498 \text{ rad s}^{-1}$, two trajectories did not separate until at least $1.2 \times 10^6 \text{ s}$.

Figure 4 shows the dependency of the bifurcation diagrams of the chemical system on the α value. The bifurcation diagrams were depicted with the data on the Poincaré sections ($\cos \omega_p t = 1$). In the case that $\alpha = 0.1$, there was a quasiperiodic region (and a narrow chaotic one) between the 1/2 and 1/3 entrainment regions (Fig. 4a).¹⁶ In Fig. 4b ($\alpha = 0.12$), the quasiperiodic region has been replaced by a chaotic one, where two chaotic modes (relatively local chaos and relatively global chaos) seem to exist. This behavior is more clearly shown in Figs. 4c, 4d, and 4d', which is similar to so-called crisis.¹⁷ Any information on unstable attractors (unstable fixed points in return maps) is necessary in order to discuss the behavior. However, we could not obtain it in this computer simulation because the calculated values rapidly became unstable under the condition that $\Delta t < 0$. Figures 4d and 4d', 4e and 4e', and 4f and 4f' were obtained by using different initial values, respectively. These figures

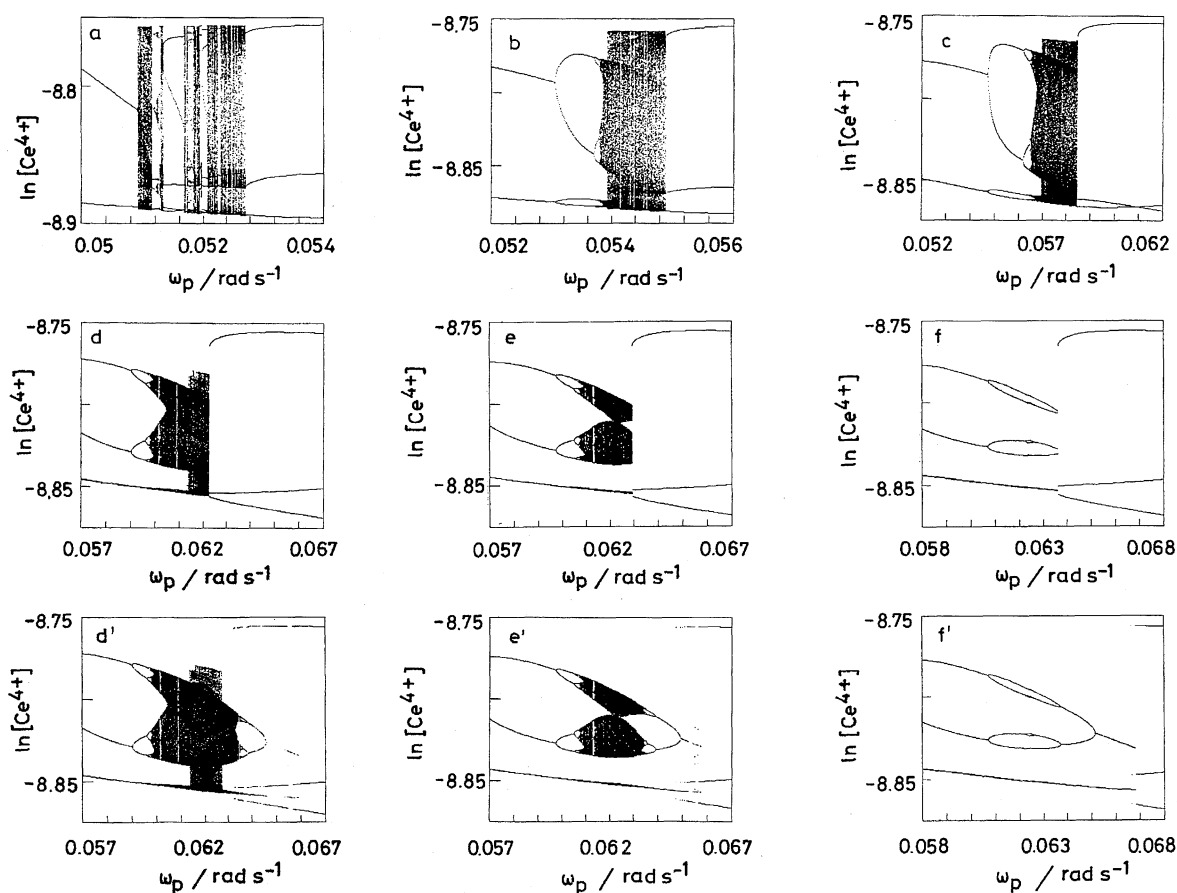


Fig. 4. Relation between the α value and the bifurcation diagram depending on the magnitude of ω_p . The CSTR condition: A. α : a, 0.1; b, 0.12; c, 0.15; d and d', 0.18; e and e', 0.185; and f and f', 0.19. The initial values are different in d and d', e and e', and f and f', respectively.

reveal that the reaction system exhibits the coexistence of the 1/3 harmonic mode and another oscillatory mode, such as chaotic and 1/2 harmonic ones, and the coexisting region is depicted with a striped pattern in Fig. 1. Determining the striped regions under the condition $\alpha < 0.18$ was very difficult because adequate initial values were not easily found. The 1/3 harmonic mode exhibited to relatively large-amplitude oscillations and the coexisting harmonic modes exhibited relatively small-amplitude oscillations. The latter harmonic modes grew into 1/1 harmonic oscillations with a small amplitude as the α value increased.¹² Figures 5a and 5b show trajectories under the condition that $\alpha = 0.18$ and $\omega_p = 0.063 \text{ rad s}^{-1}$, where one representative point was attracted into a 1/3 harmonic attractor and another into a chaotic attractor. We can imagine two basins in the seven-dimensional phase space. Of course, one basin may be bounded. However, the basins could not be made a distinction in three-dimensional phase space. On the other hand, return maps of these attractors (Figs. 5a' and 5b') showed a distinct difference. Namely, the range of the orbit of the chaotic mode was rather small, which was commonly observed in the attractors of type 2 (the 1/2 and the 1/4 harmonic modes, etc.).¹² (We should note that a range of orbits in a return map does not generally relate to the amplitude of oscillations.) An example of the coexistence of two oscillatory modes and of the existence of two chaotic modes is given by using a one-dimensional dynamical system based on a piecewise linear map in Appendix.

Chaos of Type II. Figure 6 shows a phase diagram on the chaos of type II in the ω_p - α plane.¹⁸ Some chaotic regions appeared when the fundamental 1/1 and the fundamental 1/2 entrainment regions came into contact with each other. The chaotic regions were not in contact with any quasiperiodic regions.

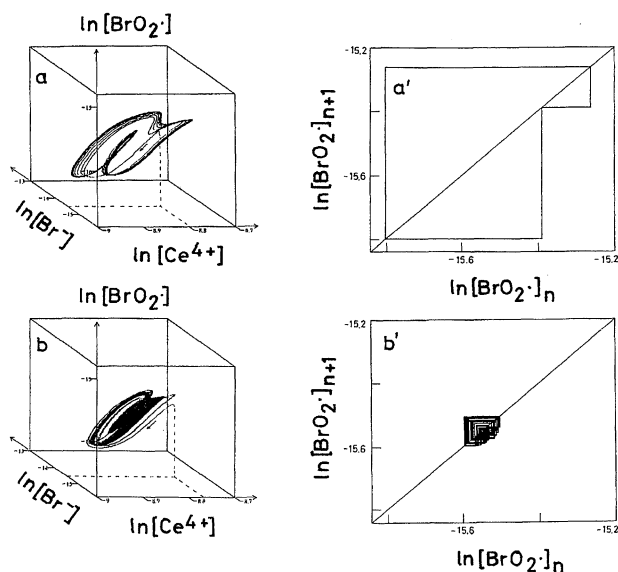


Fig. 5. Coexistence of the 1/3 harmonic mode and the chaotic mode. The CSTR condition: A. $\alpha = 0.18$ and $\omega_p = 0.063 \text{ rad s}^{-1}$. a (trajectory) and a' (return map of the attractor): 1/3 harmonic mode. b and b': chaotic mode.

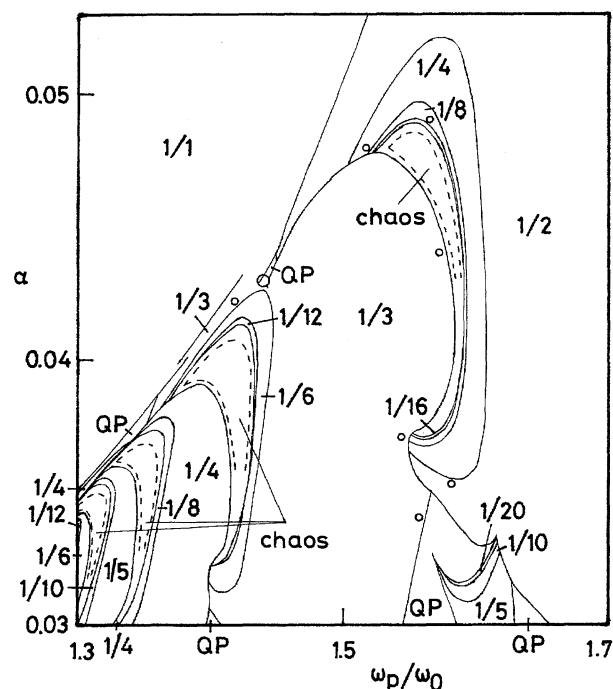


Fig. 6. Phase diagram on the chaos (type II) of the minimal chemical oscillator in the ω_p - α space. The CSTR condition: B ($[\text{BrO}_3^-]_0 = 0.12 \text{ M}$, and $k_0 = 0.0064 \text{ s}^{-1}$). QP: quasiperiodic oscillations.

The behaviors of the reaction system under the condition that $\alpha = 0.036$ are shown in Figs. 7 and 8 as a typical example. On the basis of the bifurcation diagram (Fig. 7a) and the assignments of the oscillations of $[\text{Ce}^{4+}]$ by means of Fourier spectra, Poincaré sections ($\cos \omega_p t = 1$) and return maps (the other figures), it was concluded that the state of the reaction system changed along with an increase of the ω_p value in the following manner: 1/1 (1/1) \rightarrow QS \rightarrow 1/4 (4/4) \rightarrow period-doubling bifurcations \rightarrow chaos \rightarrow reversed period-doubling bifurcations \rightarrow 1/4 (3/4) \rightarrow chaos \rightarrow reversed period-doubling bifurcations \rightarrow 1/3 (2/3) \rightarrow 1/2 (1/2) \rightarrow 1/2² ((1/2) \times (2/2)) \rightarrow 1/2 (1/2), where QS represents a quasiperiodic state and the numbers in the parentheses are winding numbers. The former chaos was created between 1/4 (4/4) (Fig. 7b) and 1/4 (3/4) (Fig. 7c) harmonic modes (generally between 1/n (n/n) and 1/n ((n-1)/n) harmonic modes), which is one of the characteristics of this chaos. (The 1/4 harmonic modes are different, as shown in Figs. 7b' and 7c'.) The quasiperiodic range between the 1/1 harmonic mode and the 1/4 (4/4) harmonic one (Figs. 8a and 8a') was generated through a Hopf bifurcation of the 1/1 harmonic oscillations. Hopf bifurcations which did not lead to doubling periods were often simulated in this system. As another example, a 1/3 (3/3) harmonic mode occurred through the bifurcation under the condition that $\alpha = 0.4$ (Fig. 6).¹⁹ The chaotic oscillations under the conditions that $\omega_p = 0.0337$ and $0.03565 \text{ rad s}^{-1}$ are shown in Figs. 8b, 8b', 8c, and 8c'. These examples of chaos were obtained through successive period-doubling bifurcations and an intermittent route. In contrast to the chaos of type I, in which the collapse of a torus and corru-

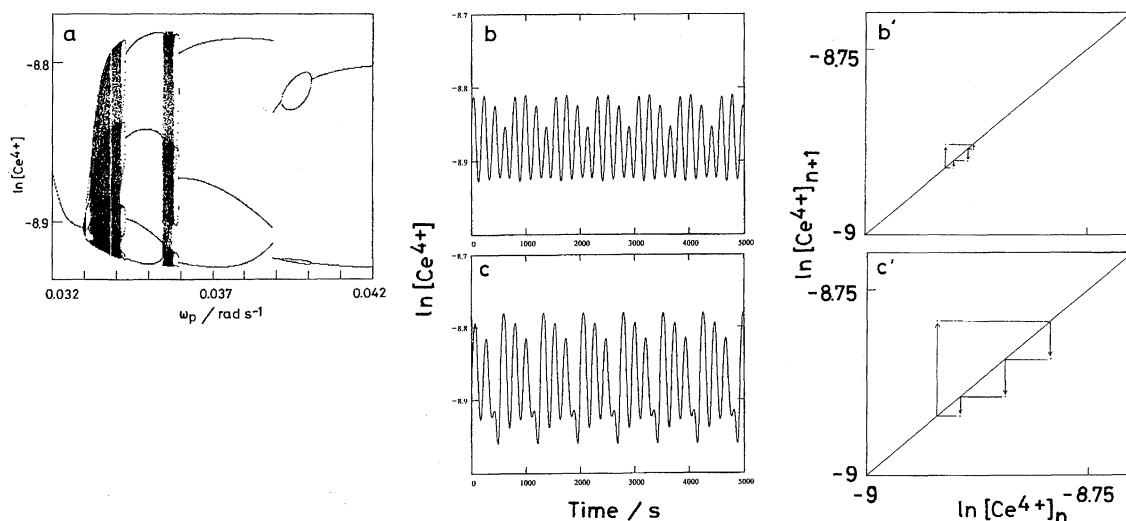


Fig. 7. Example of the route to the chaos of type II. The CSTR condition: B. $\alpha = 0.036$. a: bifurcation diagram depending on the magnitude of ω_p . b (oscillation pattern of $[\text{Ce}^{4+}]$) and b' (return map): $\omega_p = 0.03312 \text{ rad s}^{-1}$. c and c': $\omega_p = 0.0343 \text{ rad s}^{-1}$.

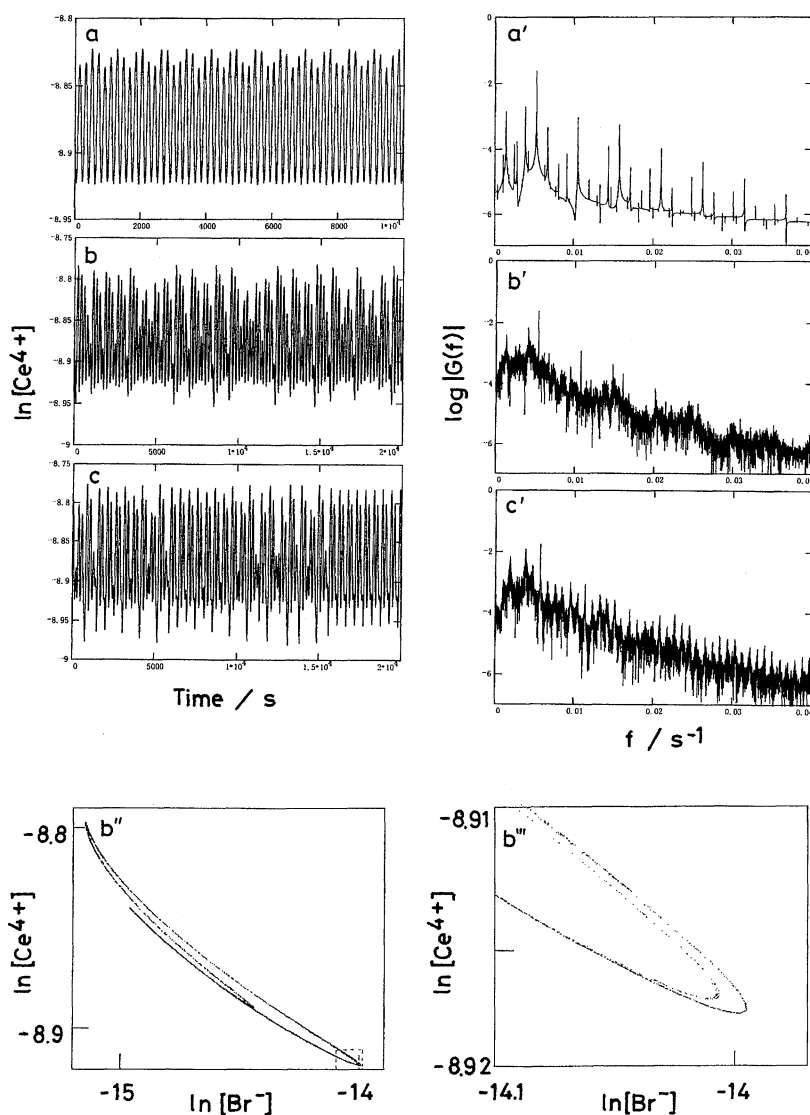


Fig. 8. Characteristics of the chaos in Fig. 7. The CSTR condition: B. $\alpha = 0.036$. a (oscillation pattern of $[\text{Ce}^{4+}]$) and a' (Fourier spectrum): $\omega_p = 0.033$. b, b', b'', and b''' (Poincaré sections ($\cos \omega_p t = 1$)): $\omega_p = 0.0337$. c and c': $\omega_p = 0.03565$. The unit of the ω_p values is rad s^{-1} .

gations on the Poincaré section were observed, the Poincaré section in Fig. 8b''' seemed to be trebly constituted. We might recognize a random alternation of 1/4 (4/4) and 1/4 (3/4) harmonic oscillations in the oscillation pattern of $[\text{Ce}^{4+}]$ (Fig. 8b) and that of 1/4 (3/4) and 1/3 (2/3) harmonic oscillations in Fig. 8c. Such a characteristic of chaotic oscillations has been observed in an Onchidium pacemaker neuron stimulated electrically.⁵

In this and previous papers, we have sketched a global profile on the response of the minimal chemical oscillator to a periodic perturbation.¹² The behaviors occurring under weakly perturbed conditions (entrainments, quasiperiodic oscillations, the Farey tree, and Arnol'd tongues) are qualitatively consistent with those estimated in the minimal oscillator²⁰ and those observed in other reaction systems.^{7,21} As the perturbation (α value) increased, the chaos of type II was first created and was followed by the chaos of type I. The small-amplitude oscillations, which were simulated under strongly perturbed conditions, have been observed experimentally.²⁰ The 1/1 harmonic mode coexisting with the 1/3 harmonic mode may be a seed of the small-amplitude oscillations.

We often encountered slowing-down periods when the oscillatory mode changed (for example in the regions of successive period-doubling bifurcations). When slowing down occurred, many calculation times (3×10^5 s at maximum) were needed until a representative point arrived at an attractor (usually less than 10^4 s). Slowing down in an experiment (slow change in the Fourier spectrum with time) has been observed at entrainment edges in a forced BZ reaction system.²² We do not know at present whether the both slowing-down periods are the same or not. Moreover, we wish to point out that there are some points where curious data are obtained (for example irregular dots under the conditions that $\omega_p = 0.0655 \text{ rad s}^{-1}$ in Fig. 4e' and at the circle points in Fig. 6). The appearance of the dots seems to be dependent upon the initial values. We do not understand the reason why such results, which are similar to transient chaos, were obtained.^{17,23}

Appendix

It seems to be difficult to understand the chaotic behaviors of the minimal oscillator on the basis of the differential equations used here because of their complicated nature. Therefore, we think that the results obtained in this study may be compared with those obtained in simple maps (piecewise linear map and cubic map).

In a piecewise linear map (circle map), n -periodic (n : integer) and quasiperiodic modes are easily obtained and chaotic regions, which are not in contact with any quasiperiodic regions, are simulated in a parameter space.²⁴ Relatively large chaos and relatively small chaos are also obtained in special cases. In a cubic map (interval map), the coexistence of two modes (1-period and chaos, 1-period and 3-period, etc.) is easily produced. Therefore, we may be able to hit upon many mathematical models concerned with the behaviors of the forced minimal oscillator, particularly the coexistence of two harmonic modes and the existence of two chaotic modes. For example we discuss a piecewise linear map shown in Fig. 9a. In order to simplify the discussion it is assumed that the map has one

parameter (b_3 , its range: 0.32–0.42) and that the map form is given as follow:

$$h(x) = \begin{cases} -2x + 0.7 & \text{if } 0 \leq x \leq 0.1 & (l_1 \text{ in Fig. 9a}) \\ -(30/19)x + 12.5/19 & \text{if } 0.1 \leq x \leq 0.29 & (l_2 \text{ in Fig. 9a}) \\ (19/6)x - 4.31/6 & \text{if } 0.29 \leq x \leq 0.35 & (l_3 \text{ in Fig. 9a}) \\ (2b_3 - 0.78)(x - 0.35)/(b_3 - 0.3) + 0.39 & & \\ 2x - 0.4 & \text{if } 0.35 \leq x \leq (b_3 + 0.4)/2 & (l_4 \text{ in Fig. 9a}) \\ 2x - 1.4 & \text{if } (b_3 + 0.4)/2 \leq x \leq 0.7 & (l_5 \text{ in Fig. 9a}) \\ 0.05 & \text{if } 0.7 \leq x \leq 0.725 & (l_5' \text{ in Fig. 9a}) \\ 0.05 & \text{if } 0.725 \leq x \leq 0.825 & (l_6 \text{ in Fig. 9a}) \\ -2x + 1.7 & \text{if } 0.825 \leq x \leq 0.85 & (l_1' \text{ in Fig. 9a}) \\ -2x + 2.7 & \text{if } 0.85 \leq x \leq 1 & (l_1'' \text{ in Fig. 9a}) \end{cases} \quad (2)$$

Thus the map is

$$x_{n+1} = h(x_n) \quad (n = 0 \text{ or integer}). \quad (3)$$

The $h(x)$ value at the intersecting point between line l_5 and the diagonal is 0.4 (b_0) and that between line l_3 and the diagonal is 4.31/13 (b_1). $h(0.2) = 6.5/19$ (b_2). Thus, we obtain $b_1 < b_2 < 0.39 < b_0$. As shown in Fig. 9a, the map possesses a stable 3-period orbit. Bifurcation diagrams are shown in Figs. 9b and 9b', where the initial values are different. The broken curves in Fig. 9b represent unstable fixed points. When $0 < x < 4.9/30$ (x'_0) and 0.4 (x'_1) $< x < 1$, the map displays a relatively large 3-period all over the range of b_3 . On the other hand, the map displays relatively large chaos, relatively small chaos, 2-period, 1-period, and relatively large 3-period when $x'_0 < x < x'_1$. When $b_3 = 0.4$, a tangent bifurcation occurs and an unstable fixed point is created. When $b_3 = b_1$, a transition between the relatively large chaos and the small one (interior crisis) occurs.¹⁷ The change of a circle map to an interval map along with an increase (or a decrease) of a parameter remains as an interesting problem.²⁵

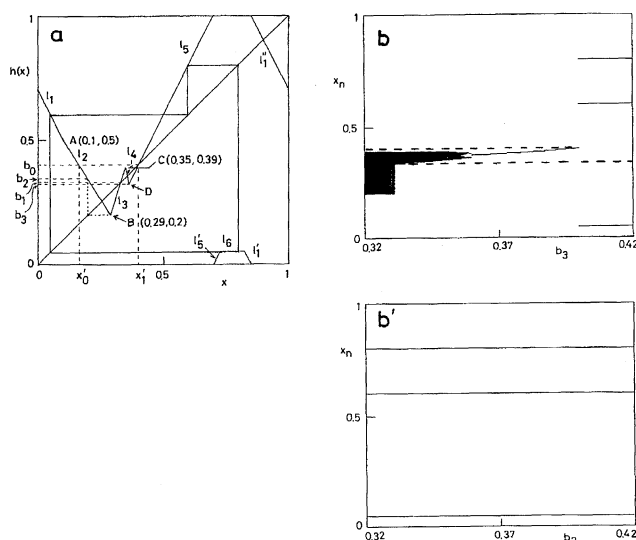


Fig. 9. A piecewise linear map concerning the coexistence of 3-period mode and other modes such as chaotic and 1-period modes. a: piecewise linear map. b and b': bifurcation diagrams depending on the magnitude of b_3 . The initial values are different in b and b'. The broken curves in b represent unstable fixed points.

References

- 1 I. R. Epstein and K. Showalter, *J. Phys. Chem.*, **100**, 13132 (1996). See references cited therein.
- 2 M. J. B. Hauser and L. F. Olsen, *J. Chem. Soc., Faraday Trans.*, **92**, 2857 (1996).
- 3 T. Hauck and F. W. Schneider, *J. Phys. Chem.*, **97**, 391 (1993).
- 4 T. Kai and K. Tomita, *Prog. Theor. Phys.*, **61**, 54 (1979).
- 5 H. Hayashi, S. Ishizuka, and K. Hirakawa, *J. Phys. Soc. Jpn.*, **54**, 2337 (1985).
- 6 K. Aihara, G. Matsumoto, and M. Ichikawa, *Phys. Lett. A*, **111**, 251 (1985).
- 7 M. Dolnik, J. Finkeová, I. Schreiber, and M. Marek, *J. Phys. Chem.*, **93**, 2764 (1989).
- 8 R. J. Field, E. Körös, and R. M. Noyes, *J. Am. Chem. Soc.*, **94**, 8649 (1972).
- 9 W. Geiseler and K. Bar-Eli, *J. Phys. Chem.*, **85**, 908 (1981).
- 10 W. Hohmann, J. Müller, and F. W. Schneider, *J. Phys. Chem.*, **100**, 5388 (1996).
- 11 A. Kaminaga and I. Hanasaki, *J. Phys. Chem.*, **102**, 3307 (1998).
- 12 Y. Sasaki, *Bull. Chem. Soc. Jpn.*, **72**, 1465 (1999).
- 13 R. J. Field and H.-D. Försterling, *J. Phys. Chem.*, **90**, 5400 (1986).
- 14 P. Bergé, Y. Pomeau, and C. Vidal, "Order within chaos — Towards a Deterministic Approach to Turbulence," John Wiley & Sons, Inc., New York (1984).
- 15 In this calculation and in similar calculations described later the difference of the initial values of $[\text{Br}^-]$ ($\Delta[\text{Br}^-]_{\text{ini}}$) is 10^{-9} mol dm $^{-3}$ and the initial values of the other variables are fixed. The ratio of $\Delta[\text{Br}^-]_{\text{ini}}$ to $[\text{Br}^-]_{\text{ss}}$ is 0.2%, where $[\text{Br}^-]_{\text{ss}}$ represents the concentration of Br^- in the unstable steady state under the condition A (Table 2).
- 16 Here we assigned an obscure chaotic state to a quasiperiodic one.
- 17 C. Grebogi, E. Ott, and J. A. Yorke, *Physica*, **7D**, 181 (1983).
- 18 We did not obtain closed curves in parts of 1/3 harmonic and quasiperiodic mode regions because of the coexistence of different harmonic modes.
- 19 The quasiperiodic and the period-tripling bifurcations seem to be special cases of Hopf bifurcation. In a quasiperiodic Hopf bifurcation a representative point in a Poincaré section rotates irrationally on a unit circle if we assume two-dimensional nonlinear equations. Therefore, this quasiperiodicity should be distinguished from that generated under weakly perturbed conditions. See: R. L. Devaney, "An Introduction to Chaotic Dynamical Systems," Benjamin/Cummings Publishing, Menlo Park (1986).
- 20 T. W. Taylor and W. Geiseler, *Ber. Bunsenges. Phys. Chem.*, **89**, 441 (1985).
- 21 A. Karantonis, M. Pagitsas, and D. Sazou, *Chaos*, **3**, 243 (1993).
- 22 F. Buchholz, A. Freund, and F. W. Schneider, "Temporal Order," ed by L. Rensing and N. I. Jaeger, Springer-Verlag, Berlin (1985), p. 116.
- 23 J. L. Kaplan and J. A. Yorke, *Commun. Math. Phys.*, **67**, 93 (1979).
- 24 For example the behaviors of piecewise linear maps are reported in the following papers: B. Christiansen, P. Alstrøm, and M. T. Livinsen, *Phys. Rev. A*, **42**, 1891 (1990), and D. K. Campbell, R. Galeeva, and D. J. Uherka, *Chaos*, **6**, 121 (1996).
- 25 It is reported that such a change occurs along with an increase of perturbation in a kicked oscillator. E. J. Ding, *Phys. Rev. A*, **A35**, 2669 (1987).